The MHC class-II HLA-DR receptor mediates bat influenza A-like H17N10 virus entry into mammalian cells

Efstathios S Giotis[1*], George Carnell[2, 3], Erik F. Young[4 †], Saleena Ghanny[4 ††], Patricia Soteropoulos[4 ††], Wendy S Barclay[1], Michael A Skinner[1], Nigel Temperton[2]

[1]Section of Virology, Department of Medicine, St Mary's Campus, Imperial College London, UK.

[2]Viral Pseudotype Unit, Medway School of Pharmacy, University of Kent and University of Greenwich, Chatham Maritime, UK.

[3]Laboratory of Viral Zoonotics, Department of Veterinary Medicine, University of Cambridge, UK.

[4]Hackensack University Medical Centre Department of Surgery, Hackensack, NJ.

Current affiliations:

[†]Bioelectronic Systems Lab, Columbia University, NY, USA.

[††]University of Medicine and Dentistry of New Jersey, Centre for Applied Genomics, Newark, NJ, USA.

*Corresponding author: Efstathios S Giotis e.giotis@imperial.ac.uk

Abstract:

Bats are notorious reservoirs of diverse, potentially zoonotic viruses, exemplified by the evolutionarily distinct, influenza A-like viruses H17N10 and H18N11 (BatIVs). The surface glycoproteins [haemagglutinin (H) and neuraminidase (N)] of BatIVs neither bind nor cleave sialic acid receptors, which suggests that these viruses employ cell attachment and entry mechanisms that differ from those of classical influenza A viruses (IAVs). Identifying the cellular factors that mediate entry and determine susceptibility to infection will help assess the host range of BatIVs. Here, we investigated a range of cell lines from different species for

their susceptibility to infection by pseudotyped viruses (PV) bearing bat H17 and/or N10 envelope glycoproteins. We show that a number of human haematopoietic cancer cell lines and the canine kidney MDCK II (but not MDCK I) cells are susceptible to H17-pseudotypes (H17-PV). We observed with microarrays and qRT-PCR that the dog leukocyte antigen DLA-DRA mRNA is over expressed in late passaged parental MDCK and commercial MDCK II cells, compared to early passaged parental MDCK and MDCK I cells, respectively. The human orthologue HLA-DRA encodes the alpha subunit of the MHC class II HLA-DR antigen-binding heterodimer. Small interfering RNA- or neutralizing antibody-targeting HLA-DRA, drastically reduced the susceptibility of Raji B cells to H17-PV. Conversely, over expression of HLA-DRA and its paralogue HLA-DRB1 on the surface of the unsusceptible HEK293T/17 cells conferred susceptibility to H17-PV. The identification of HLA-DR as an H17N10 entry mediator will contribute to a better understanding of the tropism of the virus and will elucidate its zoonotic transmission.

Keywords: influenza, bats, pseudotype virus, MHC-class II, HLA-DR

Abbreviations: SARS: severe acute respiratory syndrome; MERS: Middle-East respiratory syndrome; CoV: coronavirus; MDCK: Madin-Darby canine kidney cells; HIV: human immunodeficiency virus; CD4: cluster of differentiation 4; MHC: Major histocompatibility complex; ATCC: American type culture collection; gag: group-specific antigen; pol: polymerase; SEM: standard error of the mean.

Main:

Outbreaks of SARS, MERS, Nipah and Ebola have highlighted the critical need to focus on the zoonotic potential of known, and novel, bat viruses to improve forecasting, prevention and control of epidemics. Viral diversity in bats is exemplified by the discovery of the enigmatic

influenza A-like viruses (BatIVs) H17N10 and H18N11 in asymptomatic New World bats (*Sturnira lilium* and *Artibeus planirostris* respectively)[1, 2] and more recently by the detection of a virus related to avian H9N2 in Egyptian *Rousettus aegyptiacus* bats[3]. Such discoveries prompted investigation of the pandemic potential of these viruses and led to concern that bats may be a neglected reservoir of novel influenza viruses[4].

Influenza A viruses (IAVs) are enveloped orthomyxoviruses with eight single-stranded negative-sense viral RNAs (vRNAs) encapsidated into viral ribonucleoproteins (vRNPs). The original source of classical IAVs is aquatic birds, from which they emerge, *via* genome reassortment and mutation, to cause sporadic pandemics in humans, lower animals and other birds[5, 6]. They are classified into different subtypes based on their envelope glycoproteins (trimeric haemagglutinin, HA: H1-H18, and tetrameric neuraminidase, NA: N1-N11)[7]. HA is synthesised as a precursor protein in infected cells and its cleavage by host cell proteases sets in motion a complex series of events that is initiated by receptor binding and is terminated with the penetration of the virus into the cytoplasm of target cells[8]. HA conventionally attaches to host-specific sialic acid (SA) moieties[6]. These are terminal sugars of larger carbohydrate chains attached to the cell membrane by the lipids or proteins that they decorate. When HA attaches to them, it triggers endocytosis of the virus into membrane bound endosomes[9, 10]. Acidification of the endosome induces conformational changes to HA, which lead sequentially to: insertion of the hydrophobic "HA fusion peptide" into the host membrane, juxtaposition of the viral and endosomal membranes and subsequent release of the vRNPs into the cytoplasm via a fusion pore[11, 12]. In contrast, NAs are glycosidases which primarily cleave cell surface SA and therefore facilitate the release and spread of virus progeny upon egress, as well as disaggregation of virions before entry[13, 14].

The crystal structures of BatIV HAs and NAs revealed divergence of their protein conformations from those of conventional IAVs, suggesting distinct binding and functional properties[2, 15, 16, 17]. Bat H17 and H18 proteins have typical HA folds but lack an obvious cavity

to accommodate SA[2, 15, 17]. The cell receptors for the BatIVs are as yet unidentified, but they are clearly not SA moieties, a conclusion reached by several studies[15, 18, 19]. Furthermore, bat N10 and N11 are structurally similar to classical NAs but lack conserved amino acids for SA binding and cleavage[2, 16, 17] and do not exhibit typical neuraminidase activity[18, 20]. Initial efforts to isolate infectious BatIVs directly from bats have failed, mainly because the receptors were unknown and susceptible cell lines were unavailable[21, 22, 23]. Attempts to circumvent these limitations have included H17- or H18-pseudotyped vesicular stomatitis virus (VSV[19, 24]), engineered BatIV/IAV chimeric viruses[23, 25], and authentic BatIVs reconstructed using reverse genetics[26]. H17-VSV was able to infect bat cell lines (EidNi, HypNi, and EpoNi) but only a few, common cell lines of flightless mammals, including some of human (U-87 MG glioblastoma and SK-Mel-28 melanoma) and canine (RIE1495 and MDCK II kidney) origin[19, 24, 26]. These cells could also be infected with reconstructed H17N10 and H18N11 viruses[26]. The ability of BatIVs to infect mammalian cell lines *in vitro*, and their unconventional features, raised concerns about their zoonotic and epidemic potential. Identifying the BatIV cell surface receptors and delineating the mechanistic basis of the host-virus interaction are key to assessing their potential host range and public health significance.

HIV-1 derived-pseudotypes bearing heterologous envelope proteins (PV) have been used widely for the assessment of cellular tropism and the identification of cellular receptors or attachment factors for a range of viruses[27, 28, 29, 30, 31]. Such pseudotypes have proved a reliable model to study the capacity of H17N10 for entry into various cell lines[27, 32]. Using this approach, we have shown that H17-PV, and H17N10-PV (A/little yellow-shouldered bat/Guatemala/060/2011) are recovered from producer HEK293T/17 cells exclusively in the presence of the human airway trypsin-like protease (HAT) or the transmembrane protease, serine 2 (TMPRSS2) (Fig. 1a)[32]. In this study, a panel (n=35; Supplementary material 1) of cell lines from different tissues and species were challenged with H17- and/or N10–PV to study

the distribution of the H17N10 receptor(s) (Fig. 1b). Efficiency of infections with PV was quantified (after 48 h) by the expression of a firefly luciferase (FLuc) reporter gene encoded by the lentiviral genome. Parallel infections were conducted with PV bearing either classical H5 (H5-PV; A/Vietnam/1194/2004; H5N1 clade 1) or VSV-G (VSV-G-PV) glycoproteins (the latter displaying very broad tropism) as positive controls to eliminate possible post-binding blockage factors. HIV particles produced in the absence of a viral envelope protein (Δ-env) served as a negative control. H17-PV displayed highly limited host and species cell tropism, suggesting that the H17 cellular receptor(s) are not ubiquitous (Fig. 1b). Of note, the bat cell lines (lung & kidney) from *S. lilium* in which H17N10 was discovered, were not susceptible to PV. This implies that expression of the H17-putative receptor(s) and/or viral entry-related host factors was either lost during immortalisation or is tissue-type restricted. Conversely, we show that the dog epithelial kidney MDCK II (unlike MDCK I) cells are susceptible to H17-PV with titers comparable to those of control VSV-G- and H5-PV in the range of 10^6 to 10^7 RLU/ml (Fig. 1c). They were not susceptible to PV expressing N10 alone and co-expression of N10 with H17 did not improve infection of MDCK II (Fig. 1c), which suggests that N10 has a dispensable role in viral entry (*in vitro)*. To characterise the H17 putative receptors, MDCK II cells were either pre-treated with neuraminidase, tunicamycin or pronase or treated with ammonium chloride before infection with H17-PV. Infectivity with H17- and H5-PVs, as well as cytotoxicity (by trypan blue exclusion), were assayed 24 h post treatment (Fig. 1d). Pre-treatment of MDCK II cells with neuraminidase from *Clostridium perfrigens* (1-100 mU), which cleaves cell surface SA, reduced H5-PV infection by 68-86% but did not significantly affect infection by H17-PV, supporting the notion that SA are not the cell surface receptors for H17[19, 26]. Classical IAVs primarily enter cells via endocytosis followed by endosomal fusion triggered by low pH. Treatment of MDCK II cells with the pH neutralising agent ammonium chloride (1-100 mM) abolished luciferase activity for both H5- and H17-PV, demonstrating that entry of H17, like IAVs, into target cells is pH-dependent. Similar results were obtained in

RIE1495 cells[32]. Entry of H17-PV was more susceptible to pre-treatment of MDCK II cells with proteases or tunicamycin (an inhibitor of *N*-glycosylation) than was entry of H5-PV (being reduced by up to 72 and 78%, compared to 45 and 20%, respectively), suggesting that the H17-cellular receptor(s) may be a glycosylated protein, in line with previous proposals[19].

MDCK I and II represent early and late passaged cells from the same parental NBL-2 cell line (CCL-34, ATCC). MDCK are valuable cell lines in studies of viruses, cell-cell junctions and epithelial differentiation but consist of heterogeneous cell populations and their phenotypes vary significantly between user laboratories[33]. In addressing the factors that permit infection of H17-PV in late passaged MDCK II cells, we considered that parental NBL-2 cells undergo passage number-dependent phenotypic changes that may be reflected at transcriptional level. The phenotypic transition of NBL-2 cells to early and late MDCK cells was investigated using the Affymetrix canine microarray 2.0 (E-GEOD-14837; passages 8 and 21 respectively). The microarray analysis identified 17 differentially regulated transcripts: 12 up-regulated and 5 down-regulated in late- compared to early-passaged cells (Fig. 2a). The current prevalent hypothesis is that single or multiple cell surface molecules are essential for the initial attachment and uptake of enveloped viruses into cells[34, 35]. Therefore, we surveyed the differentially regulated transcripts for encoded, surface-anchored proteins using a combined analysis of: available Gene Ontology annotations, existing literature as well as transmembrane protein domain and subcellular localisation prediction algorithms (Phobius, TMHMM and DeepLoc). The analysis identified the dog leukocyte antigen class II DR α-chain (DLA-DRA) as the only transcript, encoding a membrane protein, over-expressed in late, compared to early, passage MDCK cells (full data in Supplementary material 2). Significant over-expression of DLA-DRA (and its paralogue DLA-DRB1) was also confirmed (by qRT-PCR) in MDCK II compared to MDCK I cells (Fig. 2b).

157 DLA-DRA is a well-conserved orthologue of the human leukocyte antigen class II DR α-chain
158 (HLA-DRA) (~90% amino acid identity between canine, human and *Desmodus rotundus* bat
159 ectodomains; Supplementary material 3). In humans, MHC-II molecules occur as three highly
160 polymorphic isotypes (HLA-DR, HLA-DP and HLA-DQ) which are selectively expressed
161 under normal conditions on the surface of antigen presenting cells (APCs), including B,
162 dendritic and mononuclear phagocyte cells. These molecules are non-covalently associated
163 heterodimers of two glycosylated, transmembrane polypeptide chains, the monomorphic
164 35-kDa α-chain and the highly polymorphic 28-kDa β-chain[36]. Both chains have an
165 extracellular portion composed of two domains (α1 and α2, or β1 and β2) that is anchored
166 on the cell membrane by short transmembrane and cytoplasmic domains (Fig. 2c). In the
167 classical scenario, the protease-derived foreign antigen peptides bind to MHC class II proteins
168 in the cleft formed by the α1 and β1 domains, and the complex is transported to the cell
169 surface[36, 37]. When antigenic peptides are not available, endogenous peptides such as the class
170 II associated invariant peptide (CLIP) substitute them and restore MHC class II dimer
171 stability[37]. The complex of HLA-DR and endocytosed peptides (usually 9-30 amino acids in
172 length), constitutes a ligand for the T-cell receptor (TCR) and plays a key role in the
173 presentation of foreign antigens to $CD4^+$ T helper cells and immune surveillance[38, 39].
174
175 Since the ultimate goal of our studies is to obtain insight on the zoonotic potential of H17N10,
176 we focused on the possible influence of HLA-DR on cellular susceptibility to H17. Hence,
177 taking advantage of the high expression of HLA-DR on certain human hematopoietic
178 carcinomas[40], we further explored H17-PV tropism using a panel of human leukaemia and
179 lymphoma cell lines (Fig. 2d). We found that the Burkitt's lymphoma-derived Raji, Ramos and
180 BJAB B-lymphocytes and the B lymphoblastoid cells (B-LCL) show decreasing susceptibility,
181 in that order, to H17-PV. Kasumi-1 leukaemic cells showed marginal susceptibility in terms of
182 luciferase activity, while Molt-4 and HL-60 leukaemic cells, Jurkat T-cells, pro-monocytic THP-

1 and U-937 cells, and primary B cells showed no susceptibility to the pseudotypes (Fig. 2d, left Y axis). We hypothesised that the different susceptibility of the various cell types by H17-PV were due to disparate expression of HLA-DR, confirmed by qRT-PCR analysis for a non-polymorphic region of the α chain of HLA-DR on the same samples (Fig. 2d, right Y-axis). The presence of the HLA-DR heterodimer was also confirmed by flow cytometry with a FITC-conjugated monoclonal antibody (clone Tü36), which specifically binds to a monomorphic epitope on the HLA-DR α/β complex and not the isolated α or β chains (Fig. 2e)[41]. Both approaches indicate association between mRNA levels, the surface expression of HLA-DR heterodimer and susceptibility to H17-PV. Raji, BJAB and Ramos B cells were found to consist of 100% HLA-DR$^+$ cells; Kasumi-1 demonstrated a 7% subpopulation of HLA-DR$^+$ cells and MOLT-4 and HL-60 cells were 100% HLA-DR$^-$. These results were relatively constant and did not change with factors such as cell density or passage number.

To confirm the influence of HLA-DR on H17-PV entry into B cells, HLA-DR was independently suppressed by siRNA-mediated inhibition or by antibody blocking. Raji B cells were transfected twice over 48 h with an siRNA mixture specific for HLA-DRA (siHLA-DRA) or a control siRNA (siControl) and then challenged with the H17-PV for another 48 h. The efficiency of HLA-DRA knock-down was confirmed by qRT-PCR and western Blot. The mRNA and protein expression of HLA-DRA was reduced by ≥50% in Raji cells transfected with siHLA-DRA compared to those transfected with siControl. Knocking down HLA-DRA in Raji cells correspondingly reduced the infection of H17-PV by 50% (Fig. 2f).

To determine if blocking attachment of virus to the HLA-DR ectodomain can prevent its entry, Raji cells were incubated with increasing concentrations of a monoclonal antibody (mAb Clone 302CT2.3.2) targeting a monomorphic, extracellular region of the HLA-DRA antigen

(HLA-DRA epitope: amino acids 48-75). The presence of the antibody significantly reduced, in a dose-dependent manner, infection with H17-PV but not VSV-G-PV (Fig. 2g).

We next sought to ascertain whether ectopic expression of HLA-DR was sufficient to increase the susceptibility of non-APC, HEK293T/17, cells to the H17-PVs. HEK293T/17 cells were transiently transfected with the DRA expression vector, alone or in combination with DRB1. Surface expression of the α/β heterodimer was validated using immunofluorescence and flow cytometry. Expression of either DRA or DRB1 alone resulted in marginal or no increase in surface staining of HLA-DR or H17-PV infection (data not shown). In contrast, 1:1 co-expression of both DRA and DRB1 formed a functional α/β heterodimer on the cell surface in approximately 47% of the cell population (Fig. 2h and Supplementary material 4). This suggests that both α and β chains are necessary for cell-surface expression, consistent with previous studies[42, 43]. Transient over expression of HLA-DR in HEK293T/17 cells resulted in significant infection by H17-PV. Infection was higher by more than two orders of magnitude (Fig. 2i) in Fluorescence-activated cell sorting (FACS)-sorted cells enriched for HLA-DR. Further, expression of the human HLA-DR α and β chains in the bat *Pteropus alecto* kidney PakiTO3 cells allowed infection with H17-PV (Supplementary material 5).

Taken together, HLA-DR is shown to function as a *bona fide* entry mediator for H17 but may function with unknown factors that facilitate virus internalisation. Interaction between HLA-DR and H17 may trigger viral entry through canonical receptor-mediated endocytosis, but could also trigger entry through an activation of cell signalling pathways that the virus subverts to its advantage. Our finding therefore raises questions on the utility and possible evolutionary advantage(s) that an APC-associated receptor would confer to H17N10 infectivity and broader fitness. Some viruses exploit cells of the immune system, such as macrophages, B and dendritic cells, either as viral reservoirs or as “Trojan horses” to

234 penetrate the epithelial barriers[44, 45]. The measles virus for example, exploits macrophages or
235 dendritic cells, which traffic the virus to bronchus-associated lymphoid tissue or regional
236 lymph nodes, resulting in local amplification and subsequent systemic dissemination by
237 viremia[46]. A similar strategy employed by H17N10 could provide an explanation on why viral
238 RNA was detected in different organs and tissues in carrier *S. lilium* bats (i.e. lung, kidney,
239 liver, intestine) and why the virus fails to grow *in vitro* in cell lines developed from the same
240 tissues[1, 26]. The prototypic gammaherpesvirus, Epstein-Barr virus (EBV), employs resting B
241 cells as transfer vehicles for infection of epithelial cells[47], and also uses the HLA-DR (β1
242 domain) as receptor in order both to enter B cells as well as to impair antigen presentation
243 (by sterically blocking the engagement of HLA-DR1 and the TCR Vα domain)[48, 49, 50]. It is
244 possible that through efficient binding to HLA-DR, H17N10 may have developed a means of
245 simultaneously accessing lymphoid cells and blocking T-cell responses. Such an immune
246 evasion mechanism could explain, at least partially, its survival and asymptomatic status in
247 carrier bats. With limited functional information available on the bat MHC-II, the biological
248 role of the host HLA-DR orthologue in the pathogenesis and transmission mechanisms of the
249 H17N10 virus remains obscure.
250 In this study we did not establish the stoichiometry of the HLA-DR: H17 engagement, or
251 clarify how the virus moves to sub-membranous regions and might hijack the receptor-
252 mediated signalling pathway to promote its internalization. It is likely that the determinants
253 of viral entry *in vivo* are more complicated. We cannot rule out the use by H17N10 (as by
254 other bat-borne viruses, *e.g.* SARS CoV[51, 52]) of more than one molecular species as (co-)
255 receptors. Nevertheless, the implication of this study is that H17N10 has the capacity to
256 enter human HLA-DR$^+$ cells and our work provides substantial evidence that the H17N10
257 virus has zoonotic potential. The current finding not only sheds light on the understanding
258 of BatIV host range, but also provides additional information on the evolution of influenza
259 A viruses.

Materials and methods

Cell lines, cell culture and treatment

Cell lines (complete description in Supplementary material 1) were kindly provided as follows: the HEK293T/17 cells were provided by Dr Edward Wright (University of Westminster, UK); Kasumi-1, HL-60, Molt-4, Jurkat cells from Professor Paul Farrell (Imperial College London, UK); *Pteropus alecto* cell lines from Professor Linfa Wang (NUS Duke, Singapore); *Sturnira lilium, Artibeus planirostris*, and *Carolia perspicillata* cell lines have been generated in the labs of Dr Carles Martínez-Romero/Professor Adolfo Garcia-Sastre (Icahn School of Medicine, New York) from bat tissue samples originally collected by Dr Eugenia Corrales-Aguilar (University of Costa Rica); B-LCL were created by Dr Konstantinos Paschos by infecting with recombinant EBV B cells from isolated peripheral blood monocytes (PBMCs) of a healthy donor of the prototypical B95-8 background (Imperial College London); Raji, Ramos and BJAB from Dr Rob White (Imperial College London); U-937 and THP-1, BEAS-2B, Caco-2 from Dr Marcus Dorner, Dr Michael Edwards and Professor Robin Shattock respectively (Imperial College London). The rest of cell lines were either from the collection of Dr Michael Skinner or from ATCC. Primary B cells were a kind gift by Dr Rob White (Imperial College London). B cells were isolated from peripheral blood leukocyte (PBL) samples obtained from anonymous buffy coat donors (UK Blood Transfusion Service) by centrifugation over Ficoll. CD19 microbeads were used for magnetic separation of purified B cells using an autoMACS separator (Miltenyi Biotec). All cell lines in this study were cultured according to standard mammalian tissue culture protocols (ATCC; www.atcc.org). Bat cell lines were propagated in Dulbecco's modified eagle medium (DMEM) (Life Technologies) supplemented with heat-inactivated 15% fetal bovine serum (Life Technologies), penicillin (100 U/ml) and streptomycin (100 µg/ml; Invitrogen). All cells were maintained in a

humidified incubator at 37°C and 5% CO_2 and were found free of mycoplasma contamination on repeated testing with the MycoFluor Mycoplasma Detection Kit (Life Technologies, UK).

MDCK II cells were treated as previously[19] with the following modifications. MDCK II cells were either treated with the endosomal acidification reagent ammonium chloride (1, 10 or 100 mM), or pre-treated with neuraminidase from *Clostridium perfrigens* for 2 h (1, 10 or 100 mM) or pronase (a mixture of endo- and exoproteases from *Streptomyces griseus* at a final concentration of 5, 10 or 50 μg/ml; Calbiochem, UK) for 30 min, an N-glycosylation inhibitor (tunicamycin from *Streptomyces* sp. at a final concentration of 0.01, 0.1 or 1 μg/ml; Sigma-Aldrich, UK) for 5 h. Pre-treated cells were washed with phosphate buffer saline (PBS) 3 times, and then incubated/infected as before with PVs for another 24 h. Cell viabilities were assessed by a trypan blue exclusion test.

Lentiviral pseudotype virus production and susceptibility assays

Pseudotypes expressing H17 and N10 genes were produced as described previously[32, 53]. Briefly, the lentiviral packaging plasmid p8.91[54], the pCSFLW firefly luciferase lentiviral vector[55] or the GFP expressing vector pCSGW, the expression plasmids for H17 and/or N10 [vector pI.18[56] and the protease encoding plasmid pCAGGS-HAT (a kind gift by Eva Böttcher-Friebertshäuser, Philipps University of Marburg, Germany) were co-transfected using polyethylenimine transfection reagent (Sigma Aldrich, UK) into HEK293T/17 cells, plated on 6-well Nunclon© plates (Thermo Fisher Scientific, UK). Supernatants were collected 48-72 h post transfection and filtered through a 0.45 μm filter (Millipore, UK). To remove viral titer bias between different PV stocks, pseudotypes were concentrated and (re-) titrated by serial dilution. Concentration was carried out by ultra-centrifugation for 2 h at 25,000 rpm, 4°C in the SW32 rotor of a L2-65B Beckman ultra-centrifuge.

Two-fold serial dilutions of PV-containing supernatant were performed as previously described[32] using white 96-well Nunclon© plates (Thermo Fisher Scientific, UK).

Subsequently, approximately 1x10^4 (for adherent) and 3 x10^4 cells (for suspension) cells were added in 50 µl of medium per well. Plates were incubated for 48 h, after which 50 µl of Bright-Glo™ substrate (Promega, UK) was added. Luciferase readings were conducted with a luminometer (FLUOstar OPTIMA, BMG Labtech) after a 5-minute incubation period and luciferase reading recorded in relative luminescence units (RLU). Data were normalized using Δ–env and cell-only measurements and expressed as RLU/ml.

Plasmids and transfections

Mammalian expression plasmids (pcDNA3.1$^+$/C$^-$(K)DYK) for HLA-DRA (NM_019111) and HLA-DRB1 (NM_001243965) were purchased from GenScript (Piscataway, NJ; USA). HEK293T/17 cells at sub-confluence in 6-well plates or 100 mm dishes were transfected with HLA-DRA plasmid or HLA-DRB1 plasmid or a 1:1 combination of both using the Lipofectamine 3000 transfection reagent (Thermo Fisher Scientific, UK) according to manufacturer instructions. 48 h after transfection, cells were used either for immunofluorescence analysis, or for FACS analysis (cell-surface staining) or for infection with PV. Under the experimental conditions, the transfection efficiency in either plate/dish, as assessed by the GFP expression of a co-transfected GFP-expressing control plasmid, was >70% under microscopic observation. For HLA-DR stably over expressing cells, PakiTO3 cells were transfected with both HLA-DR plasmids and then selected with neomycin (500 µg/ml). Single clones were analysed for expression of the over expressed proteins.

RNA isolation for microarray analysis

Total RNA was isolated from biological triplicates of early and late passage MDCK from T25 flasks that had been seeded with 8 x 10^5 cells and allowed to become confluent and polarize over 4 days in culture cells using a Ribopure kit (Ambion, Austin, TX). Acquired RNA was precipitated with EtOH and subsequently purified employing columns, procedures and reagents from an RNEasy kit (Qiagen, Germantown, MD) and resuspended in RNAse-free H_2O. Complementary DNA and RNA synthesis were performed according to Affymetrix Expression

Analysis protocols (see www.affymetrix.com). Briefly, double-stranded cDNA was synthesized from 5 µg of total RNA using the Superscript double-stranded cDNA synthesis kit (Invitrogen). Following phenol/chloroform extraction and ethanol precipitation, a biotin-labeled in-vitro transcription reaction was carried out using the cDNA template (Enzo Life Sciences, Farmingdale, NY). Fifteen micrograms of cRNA was fragmented for hybridization to Affymetrix Canine Genome 2.0 Array GeneChips (Santa Clara, CA), which contains approximately 18,000 *C. familiaris* mRNA/EST-based transcripts and over 20,000 non-redundant predicted genes. An one-way ANOVA adjusted with the Benjamini–Hochberg multiple-testing correction [false discovery rate (FDR) of $P<0.05$] was performed with Partek Genomics Suite (v6.6 Partek) across all samples as previously[57]. Principal component analysis confirmed that batch mixing had prevented introduction of experimental bias. Comparisons were conducted between early and late passaged cells. The analysis cut off criteria were fold change ≥ ±1.5 and *P*-value ≤ 0.05. Microarray data was uploaded per MIAME standards and deposited at the GEO repository and is available under series record number GSE14837.

HLA-DRA knockdown and blocking using siRNA and monoclonal antibodies

A Sigma-Aldrich MISSION esiRNA endonuclease-derived mixture of siRNAs (EHU226621) was used to knock down HLA-DRA expression in Raji cells. Lipofectamine RNAiMAX transfection Reagent (Thermo Fisher Scientific, UK) was used to transfect exponentially grown Raji cells with 50 nM of siHLA-DRA or siRNA universal negative control (Sigma-Aldrich, UK; SIC001) according to the manufacturer's instructions. The transfection was repeated the following day and cells were collected after 48 h and either seeded at $3x10^4$ cells per well in a 96 well-plate for infection with PV or processed in order to validate siRNA activity. Total RNA and protein were collected and assessed by quantitative RT-PCR and western blot, respectively.

In order to evaluate the interaction of HLA-DR with H17 we used the HLA DRA mAb (302CT2.3.2), which is generated from mice immunized with a KLH conjugated synthetic

363 peptide between 48-75 amino acids from human HLA-DRA. After a 1 h pre-incubation with
364 increasing concentrations of the antibody in normal growth media, Raji cells ($3x10^4$) were
365 infected for 24-48 h with H17-or VSV-G-PV.
366
367 **Western blot analysis**
368 Washed cells were lysed on ice with lysis buffer [0.5% NP40 in PBS with 10 mM Tris-HCl, pH
369 7.4 supplemented with Halt Protease Inhibitor mixture EDTA-free (Thermo Fisher Scientific
370 UK)] and protein was quantified by the BCA assay kit (Thermo Fisher Scientific, UK). 20-50 μg
371 of protein was electrophoresed on a 4-15% sodium dodecylsulfate polyacrylamide gel,
372 alongside a protein ladder (Precision Plus Protein Dual Colour Standards, Bio-Rad) and
373 immunoblotted with the following antibodies using standard procedures: mouse monoclonal
374 anti-HLA-DRA (1:1000; Clone: 302CT2, Enzo Life Sciences, UK) or rabbit monoclonal a-tubulin
375 (1:2000; Cell signalling Technology, UK) antibodies. The membranes were then washed with
376 PBS for three times and incubated with goat anti-rabbit or donkey anti-mouse secondary
377 antibodies (LI-COR) in the dark for 1 h. Scanning was then carried out using the Odyssey
378 Imaging system (LI-COR).
379
380 **Immunofluorescence**
381 Transfected cells with HLA-DRA and -DRB1 expression plasmids or with the empty plasmid
382 were seeded onto glass cover slips at $5x10^4$ cells/ml in 6 well plates overnight and were fixed
383 with 4% paraformaldehyde in PBS for 30 minutes at room temperature (RT). Fixed cells were
384 washed with PBS and permeabilised with 1% Triton X-100 in PBS for 10 minutes. After
385 washing with PBS, the cover slips were incubated with a mouse HLA-DRA mAb (169-1B5.2;
386 Bio-Techne Ltd) targeting a monomorphic general framework determinant of HLA-DR Class II
387 antigen, diluted in 5% BSA/PBS for 1 hr at RT. The cover slips were then washed 3X with
388 0.02% Tween 20 and 1% BSA in PBS, followed by incubation with Alexafluor 488 conjugated

anti-mouse (Thermo Fisher Scientific, UK) for 30 minutes at RT. After washing 3X with 0.02% Tween 20 and 1% BSA in PBS, the cover slips were mounted using Prolong Gold containing DAPI (Invitrogen). Images were acquired on EVOS fluorescent microscope (EVOS FL imaging system; Life Technology, USA). Experiments were carried out twice.

Flow cytometry

For surface staining, human cancer cells and HEK293T/17 cells transfected with an empty vector or expression plasmids of HLA-DR (α and β) chains were maintained in the dark at 4°C throughout. Cells were collected, washed twice in ice-cold FACS buffer (2%FCS, 0.02% NaN_3 in PBS) and stained with a FITC-conjugated anti-human HLA-DR mAb (Clone Tü36; BD Biosciences). This antibody specifically binds to a monomorphic epitope of the HLA-DR αβ complex and not the isolated α or β chains or the HLA-DP and -DQ isotypes[41]. The cells were analyzed with BD LSR Fortressa to determine expression of HLA-DR in combination with the matched isotype control and sorted into $HLA\text{-}DR^-$ and $HLA\text{-}DR^+$ subpopulations with a FACS Aria cell sorter (BDIS, San Jose, CA, USA). The Hoechst 33342 stain was used for cell viability discrimination and the data files were analyzed using the FlowJo software (Tree Star, Inc., Sac Carlos, CA, USA). Data are representative of two independent experiments.

Relative and absolute mRNA quantification

qRT-PCR was performed on RNA samples using a two-step procedure. RNA was first reverse-transcribed into cDNA using the QuantiTect Reverse Transcription Kit (Qiagen) according to manufacturer's instructions. qRT-PCR was then conducted on the cDNA in a 384-well plate with a ABI-7900HT Fast qRT-PCR system (Applied Biosystems). Mesa Green qRT-PCR MasterMix (Eurogentec) was added to the cDNA (5 µl for every 2 µl of cDNA). The following primers were used: for canine DLA-DRA (Forward: 5'-GCTGTGGACAAAGCTAACCTTG-3', Reverse: 5'-TCTGGAGGTACATTGGTGTTCG-3'), for canine DLA-DRB1 (Forward: 5'-

AGCACCAAGTTTGACAAGC-3', Reverse: 5-AAGAGCAGACCCAGGACAAAG-3'). The following amplification conditions were used: 95°C for 5 minutes; 40 cycles of 95°C for 15 seconds, 57°C for 20 seconds, and 72°C for 20 seconds; 95°C for 15 seconds; 60°C for 15 seconds; and 95°C for 15 seconds. The output Ct values and dissociation curves were analysed using SDS v2.3 and RQ Manager v1.2 (Applied Biosystems). Gene expression data were normalized against the housekeeping gene GAPDH, and compared with the mock controls using the comparative C_T method (also referred to as the $2^{-\Delta\Delta CT}$ method[58]). Absolute copy numbers of HLA-DRA in human cell lines were calculated using a standard curve of known concentrations of the corresponding HLA-DRA cDNA expression plasmid. HLA-DRA (Forward: 5′-TCAAGGGATTGCGCAAAAGC-3′ and reverse 5′- ACACCATCACCTCCATGTGC-3′. All experiments were carried out in triplicate.

Prediction of transmembrane protein domains and subcellular topology and phylogenetic analysis

For each of the differentially regulated transcripts identified by microarrays, we used Phobius (http://phobius.sbc.su.se)[59] and TMHMM v2.0 (http://www.cbs.dtu.dk/services/TMHMM/)[60] to predict the existence of transmembrane protein domains. Similarly, we used Deeploc-1.0 (http://www.cbs.dtu.dk/services/DeepLoc/)[61] to determine sub-cellular localisation of the encoded proteins. These predictions were compared with gene annotations and literature references to confirm their reliability. The amino acid sequences of canine DLA-DRA (NP_001011723.1), human HLA-DRA (NP_061984.2), and their bat orthologues [(*Pteropus alecto* (XP_006907484.1) and *Desmodus rotundus* (XP_024413747.1)] were subjected to multiple alignment using CLC workbench 7 (CLC Bio, Qiagen, Aarhus, Denmark).

Ethics statement

The buffy coat residues for the isolation of $CD19^+$ primary B cells were purchased from the UK Blood Transfusion Service from anonymous volunteers blood donors. Therefore, no ethical approval is required.

Statistical Analyses

Graphical representation and statistical analyses were performed using Prism 8 software (GraphPad). Unless otherwise stated, results are shown as means ± SEM from three independent experiments. Differences were tested for statistical significance using one-way ANOVA with a Dunnett's or a Tukey *posthoc* test. All statistical analyses were two-sided, and $p < 0.05$ was considered statistically significant.

Acknowledgements:

Our thanks go to Jim Kaufman, Yanping Guo, Rob White, Amr Bayoumy, Ibrahim Elbusifi, Daragh Quinn and Alfred Ho for their technical assistance. This research was undertaken with the financial support of the Biotechnology and Biological Sciences Research Council (BBSRC) (http://www.bbsrc.ac.uk) via Strategic LoLa grant BB/K002465/1 "Developing Rapid Responses to Emerging Virus Infections of Poultry (DRREVIP)" and the Octoberwoman Foundation.

References:

1. Tong S, *et al.* A distinct lineage of influenza A virus from bats. *Proc Natl Acad Sci U S A* **109**, 4269-4274 (2012).

2. Tong S, *et al.* New world bats harbor diverse influenza A viruses. *PLoS Pathog* **9**, e1003657 (2013).

3. Kandeil A, *et al.* Isolation and characterization of a distinct influenza A virus from Egyptian bats. *J Virol*, (2018).

4. Brunotte L, Beer M, Horie M, Schwemmle M. Chiropteran influenza viruses: flu from bats or a relic from the past? *Curr Opin Virol* **16**, 114-119 (2016).

5. Simonsen L. The global impact of influenza on morbidity and mortality. *Vaccine* **17 Suppl 1**, S3-10 (1999).

6. Long JS, Mistry B, Haslam SM, Barclay WS. Host and viral determinants of influenza A virus species specificity. *Nat Rev Microbiol*, (2018).

7. Gamblin SJ, Skehel JJ. Influenza hemagglutinin and neuraminidase membrane glycoproteins. *J Biol Chem* **285**, 28403-28409 (2010).

8. Bertram S, Glowacka I, Steffen I, Kuhl A, Pohlmann S. Novel insights into proteolytic cleavage of influenza virus hemagglutinin. *Rev Med Virol* **20**, 298-310 (2010).

9. Lakadamyali M, Rust MJ, Zhuang X. Endocytosis of influenza viruses. *Microbes Infect* **6**, 929-936 (2004).

10. Sauter NK, *et al.* Hemagglutinins from two influenza virus variants bind to sialic acid derivatives with millimolar dissociation constants: a 500-MHz proton nuclear magnetic resonance study. *Biochemistry* **28**, 8388-8396 (1989).

11. Edinger TO, Pohl MO, Stertz S. Entry of influenza A virus: host factors and antiviral targets. *J Gen Virol* **95**, 263-277 (2014).

12. Harrison SC. Viral membrane fusion. *Nat Struct Mol Biol* **15**, 690-698 (2008).

13. Air GM, Laver WG. The neuraminidase of influenza virus. *Proteins* **6**, 341-356 (1989).

14. Matrosovich MN, Matrosovich TY, Gray T, Roberts NA, Klenk HD. Neuraminidase is important for the initiation of influenza virus infection in human airway epithelium. *J Virol* **78**, 12665-12667 (2004).

15. Sun X, *et al.* Bat-derived influenza hemagglutinin H17 does not bind canonical avian or human receptors and most likely uses a unique entry mechanism. *Cell Rep* **3**, 769-778 (2013).

16. Li Q, *et al.* Structural and functional characterization of neuraminidase-like molecule N10 derived from bat influenza A virus. *Proc Natl Acad Sci U S A* **109**, 18897-18902 (2012).

17. Zhu X, *et al.* Crystal structures of two subtype N10 neuraminidase-like proteins from bat influenza A viruses reveal a diverged putative active site. *Proc Natl Acad Sci U S A* **109**, 18903-18908 (2012).

18. Wu Y, Wu Y, Tefsen B, Shi Y, Gao GF. Bat-derived influenza-like viruses H17N10 and H18N11. *Trends Microbiol* **22**, 183-191 (2014).

19. Maruyama J, *et al.* Characterization of the glycoproteins of bat-derived influenza viruses. *Virology* **488**, 43-50 (2016).

20. Garcia-Sastre A. The neuraminidase of bat influenza viruses is not a neuraminidase. *Proc Natl Acad Sci U S A* **109**, 18635-18636 (2012).

21. Ciminski K, Thamamongood T, Zimmer G, Schwemmle M. Novel insights into bat influenza A viruses. *J Gen Virol* **98**, 2393-2400 (2017).

22. Mehle A. Unusual influenza A viruses in bats. *Viruses* **6**, 3438-3449 (2014).

23. Juozapaitis M*, et al.* An infectious bat-derived chimeric influenza virus harbouring the entry machinery of an influenza A virus. *Nat Commun* **5**, 4448 (2014).

24. Hoffmann M, Kruger N, Zmora P, Wrensch F, Herrler G, Pohlmann S. The Hemagglutinin of Bat-... *PLoS One* **11**, e0152134 (2016).

25. Zhou B*, et al.* Characterization of uncultivable bat influenza virus using a replicative synthetic virus. *PLoS Pathog* **10**, e1004420 (2014).

26. Moreira EA*, et al.* Synthetically derived bat influenza A-like viruses reveal a cell type- but not species-specific tropism. *Proc Natl Acad Sci U S A* **113**, 12797-12802 (2016).

27. Carnell GW, Ferrara F, Grehan K, Thompson CP, Temperton NJ. Pseudotype-based neutralization assays for influenza: a systematic analysis. *Front Immunol* **6**, 161 (2015).

28. Li Q, Liu Q, Huang W, Li X, Wang Y. Current status on the development of pseudoviruses for enveloped viruses. *Rev Med Virol* **28**, (2018).

29. King B, Daly J. Pseudotypes: your flexible friends. *Future Microbiol* **9**, 135-137 (2014).

30. Coakley E, Petropoulos CJ, Whitcomb JM. Assessing chemokine co-receptor usage in HIV. *Curr Opin Infect Dis* **18**, 9-15 (2005).

31. Cronin J, Zhang XY, Reiser J. Altering the tropism of lentiviral vectors through pseudotyping. *Curr Gene Ther* **5**, 387-398 (2005).

32. Carnell G*, et al.* The bat influenza H17N10 can be neutralized by broadly- neutralizing monoclonal antibodies and its neuraminidase can facilitate viral egress. bioRxiv 499947; doi: https://doi.org/10.1101/499947 (2018).

33. Dukes JD, Whitley P, Chalmers AD. The MDCK variety pack: choosing the right strain. *BMC Cell Biol* **12**, 43 (2011).

34. Nowak SA, Chou T. Mechanisms of receptor/coreceptor-mediated entry of enveloped viruses. *Biophys J* **96**, 2624-2636 (2009).

35. Byrd-Leotis L, Cummings RD, Steinhauer DA. The interplay between the host receptor and influenza virus hemagglutinin and neuraminidase. *Int J Mol Sci* **18**, (2017).

36. Kaufman JF, Auffray C, Korman AJ, Shackelford DA, Strominger J. The class II molecules of the human and murine major histocompatibility complex. *Cell* **36**, 1-13 (1984).

37. Blazekovic F*, et al.* HLA-DR peptide occupancy can be regulated with a wide variety of small molecules. *Hum Vaccin Immunother* **12**, 593-598 (2016).

38. Jones EY, Fugger L, Strominger JL, Siebold C. MHC class II proteins and disease: a structural perspective. *Nat Rev Immunol* **6**, 271-282 (2006).

39. Roche PA, Furuta K. The ins and outs of MHC class II-mediated antigen processing and presentation. *Nat Rev Immunol* **15**, 203-216 (2015).

40. Nagy ZA*, et al.* Fully human, HLA-DR-specific monoclonal antibodies efficiently induce programmed death of malignant lymphoid cells. *Nat Med* **8**, 801-807 (2002).

41. Ziegler A*, et al.* Analysis by sequential immunoprecipitations of the specificities of the monoclonal antibodies TU22, 34, 35, 36, 37, 39, 43, 58 and YD1/63. HLK directed against human HLA class II antigens. *Immunobiology* **171**, 77-92 (1986).

42. Watanabe N*, et al.* A cell-based high-throughput screening assay system for inhibitor compounds of antigen presentation by HLA class II molecule. *Sci Rep* **7**, 6798 (2017).

43. van Lith M, McEwen-Smith RM, Benham AM. HLA-DP, HLA-DQ, and HLA-DR have different requirements for invariant chain and HLA-DM. *J Biol Chem* **285**, 40800-40808 (2010).

44. Grove J, Marsh M. The cell biology of receptor-mediated virus entry. *J Cell Biol* **195**, 1071-1082 (2011).

45. Stamataki Z*, et al.* Hepatitis C virus association with peripheral blood B lymphocytes potentiates viral infection of liver-derived hepatoma cells. *Blood* **113**, 585-593 (2009).

46. Lemon K*, et al.* Early target cells of measles virus after aerosol infection of non-human primates. *PLoS Pathog* **7**, e1001263 (2011).

47. Shannon-Lowe CD, Neuhierl B, Baldwin G, Rickinson AB, Delecluse HJ. Resting B cells as a transfer vehicle for Epstein-Barr virus infection of epithelial cells. *Proc Natl Acad Sci U S A* **103**, 7065-7070 (2006).

48. Ressing ME*, et al.* Interference with T cell receptor-HLA-DR interactions by Epstein-Barr virus gp42 results in reduced T helper cell recognition. *Proc Natl Acad Sci U S A* **100**, 11583-11588 (2003).

49. Ressing ME*, et al.* Epstein-Barr virus gp42 is posttranslationally modified to produce soluble gp42 that mediates HLA class II immune evasion. *J Virol* **79**, 841-852 (2005).

50. Wiertz EJ, Devlin R, Collins HL, Ressing ME. Herpesvirus interference with major histocompatibility complex class II-restricted T-cell activation. *J Virol* **81**, 4389-4396 (2007).

51. Jeffers SA*, et al.* CD209L (L-SIGN) is a receptor for severe acute respiratory syndrome coronavirus. *Proc Natl Acad Sci U S A* **101**, 15748-15753 (2004).

52. Li W*, et al.* Angiotensin-converting enzyme 2 is a functional receptor for the SARS coronavirus. *Nature* **426**, 450-454 (2003).

53. Ferrara F, *et al.* The human Transmembrane Protease Serine 2 is necessary for the production of Group 2 influenza A virus pseudotypes. *J Mol Genet Med* **7**, 309-314 (2012).

54. Zufferey R, Nagy D, Mandel RJ, Naldini L, Trono D. Multiply attenuated lentiviral vector achieves efficient gene delivery in vivo. *Nat Biotechnol* **15**, 871-875 (1997).

55. Demaison C, *et al.* High-level transduction and gene expression in hematopoietic repopulating cells using a human immunodeficiency virus type 1-based lentiviral vector containing an internal spleen focus forming virus promoter. *Hum Gene Ther* **13**, 803-813 (2002).

56. Cox RJ, Mykkeltvedt E, Robertson J, Haaheim LR. Non-lethal viral challenge of influenza haemagglutinin and nucleoprotein DNA vaccinated mice results in reduced viral replication. *Scand J Immunol* **55**, 14-23 (2002).

57. Giotis ES, Ross CS, Robey RC, Nohturfft A, Goodbourn S, Skinner MA. Constitutively elevated levels of SOCS1 suppress innate responses in DF-1 immortalised chicken fibroblast cells. *Sci Rep* **7**, 17485 (2017).

58. Pfaffl MW. A new mathematical model for relative quantification in real-time RT-PCR. *Nucleic Acids Res* **29**, e45 (2001).

59. Kall L, Krogh A, Sonnhammer EL. Advantages of combined transmembrane topology and signal peptide prediction--the Phobius web server. *Nucleic Acids Res* **35**, W429-432 (2007).

60. Krogh A, Larsson B, von Heijne G, Sonnhammer EL. Predicting transmembrane protein topology with a hidden Markov model: application to complete genomes. *J Mol Biol* **305**, 567-580 (2001).

61. Almagro Armenteros JJ, Sonderby CK, Sonderby SK, Nielsen H, Winther O. DeepLoc: prediction of protein subcellular localization using deep learning. *Bioinformatics* **33**, 4049 (2017).

Figure legends:

Figure 1: **a.** Schematic representation of pseudotype virus production. Expression plasmids for the HIV-1 gag-pol gene, the bat H17 alone or with N10, the luciferase reporter gene with HIV-1 long tandem repeats (LTRs) and the protease gene (HAT or TMPRSS2) are generated and co-transfected into producer HEK293T/17 cells. Cells transcribe and translate the HIV-1 core genes, BatIV glycoproteins are packaged on the cell surface, and viruses bud off in an HIV-1 dependent manner. Production of N10-PV does not require co-transfection with a

protease gene. Supernatants are harvested at 48 h post-transfection and the produced pseudotype viruses (PVs) are filtered, titrated and infected into target cells. **b.** Infectivity titers of H17-PV in cells from different tissues/species [expressed in Relative Luciferase Units (RLU)/ml]. Mean luciferase activity was plotted as mean ± inter-assay deviation expressed as SEM from 3-6 independent experiments. **c.** Infectivity titers of H17-PV, N10 and control pseudotypes (VSV-G, H5 and Δ-env) in MDCK II cells. **d.** MDCK II cells were pre-treated with either neuraminidase (2 h), with pronase (30 mins) or tunicamycin (5 h) or treated with ammonium chloride, and then infected with H17-PV. Luciferase activities were measured after 24 h with a luminometer. The left Y-axis shows infection levels (% of control) and the right Y-axis shows % viability of cells related to control MDCK II cells. Experiments were carried out in triplicate.

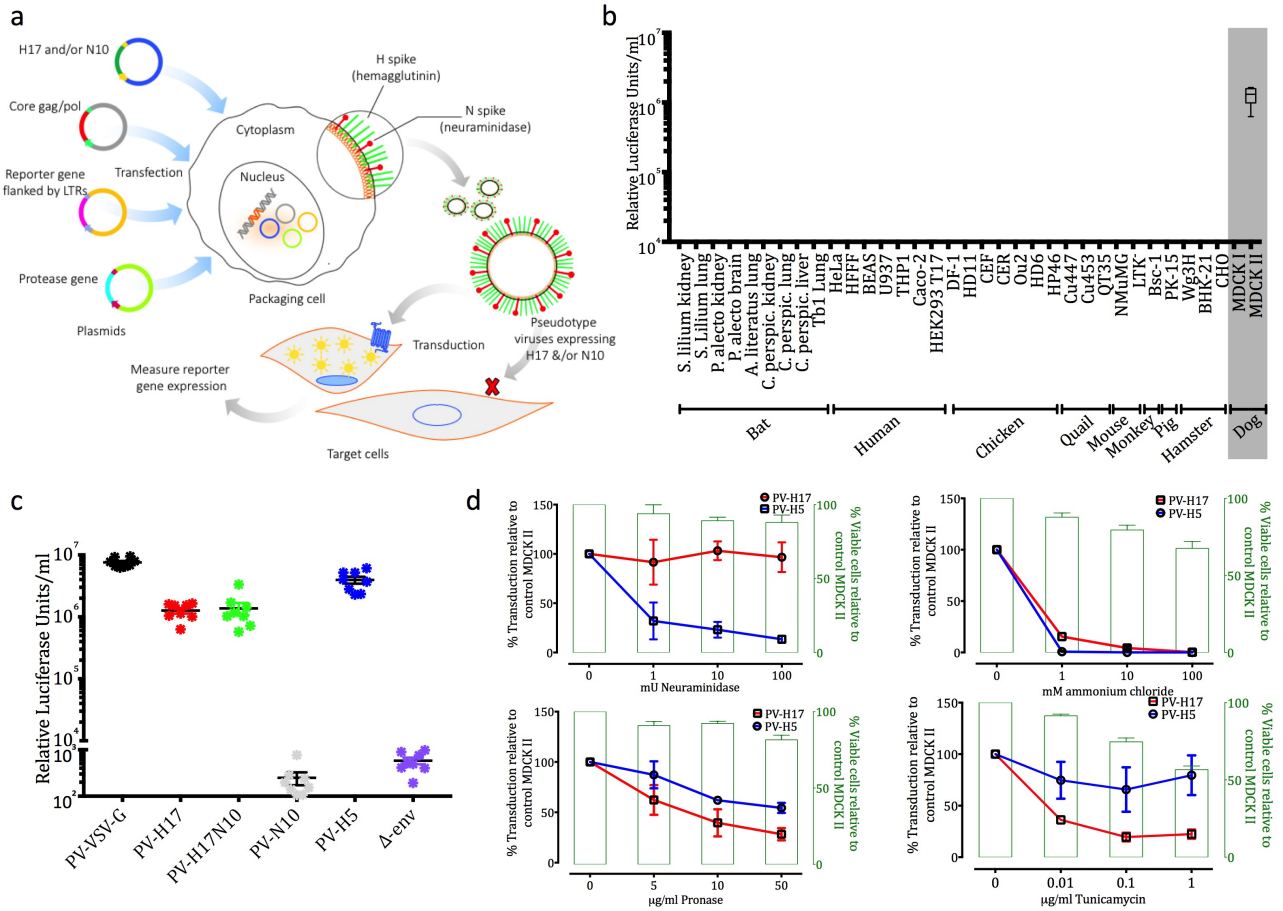

682 **Figure 2: a.** Significantly expressed genes in the microarray comparison of late versus early
683 passaged MDCK cells (green and red columns represent upregulated transcripts in MDCK II
684 and MDCK I cells respectively). Analysis was conducted with Partek (fold change ≥ 1.5 and
685 FDR ≤ 0.05)). Red frame indicates the transcript upregulated in late passaged MDCK cells
686 encoding a membrane protein. **b.** qRT-PCR results showing the expression of DLA-DRA and
687 DLA-DRB1 mRNA in MDCK I and II cells. The data are expressed as the means ± S.E.M. from
688 three independent experiments. One-way Anova with Tukey *posthoc* test were used to analyse
689 the data. ***P*<0.005 versus control. **c.** Schematic diagram of the MHC II surface molecules. **d.**
690 Left Y-axis (green box and whiskers): relative infection titers of H17-PV [$\log_{10}$ Relative
691 Luciferase Units (RLU) /ml] in a panel of human cancer cell lines. Right Y-axis (broken purple
692 line) shows $\log_{10}$ HLA-DRA mRNA copies with qRT-PCR. The data are expressed as the means
693 ± S.E.M. from three independent experiments. **e.** FACS analysis of the expression levels of cell-
694 surface HLA-DR molecule from three H17-PV susceptible and three unsusceptible cancer cell
695 lines. Results are representative from two independent experiments. Blue and read peaks
696 represent HLA-DR$^-$ and HLA-DR$^+$ subpopulations respectively. **f.** Left: infection titers of VSV-G-
697 and H17-PV (RLU/ml) in Raji cells transfected with siControl or siHLA-DRA. Right: western
698 blot (top) and qRT-PCR (bottom) showing expression of HLA-DRA protein and mRNA in
699 transfected Raji with siRNA versus siControl. Experiments were carried out twice and the
700 data are expressed as means ± S.E.M. One-way Anova with Dunnett *posthoc* test were used to
701 analyse the data. ***P*<0.005 versus siControl. **g.** Relative infection titers of VSV-G- and H17-PV
702 (RLU/ml) in Raji cells incubated with different concentrations of a monoclonal antibody
703 targeting HLA-DRA. The data are expressed as the means ± S.E.M. from three independent
704 experiments. **h.** FACS analysis of the expression levels of cell-surface HLA-DR heterodimer in
705 transiently transfected HEK293T/17 cells for 48 h with expression vectors for DRA and DRB1
706 (1:1 ratio)**.** Right hand corner microscopy picture (80x) shows immunofluorescence
707 confirming surface expression of HLA-DR on cells (green stain: FITC-HLA-DR and blue: DAPI).

The data are representative from two independent experiments. **i.** Relative infection titers of VSV-G- and H17-PV [in log10 Relative Luciferase Units (RLU) /ml] in FACS-sorted DR$^-$ HEK293T/17 cells, unsorted transiently transfected (DR$^+$ & DR$^-$) and FACS-sorted DR$^+$ cells. Experiments were carried out twice and the data are expressed as the means ± S.E.M. One-way Anova with Dunnett *posthoc* test were used to analyse the data. $^{**}P<0.005$ versus DR$^-$ cells.

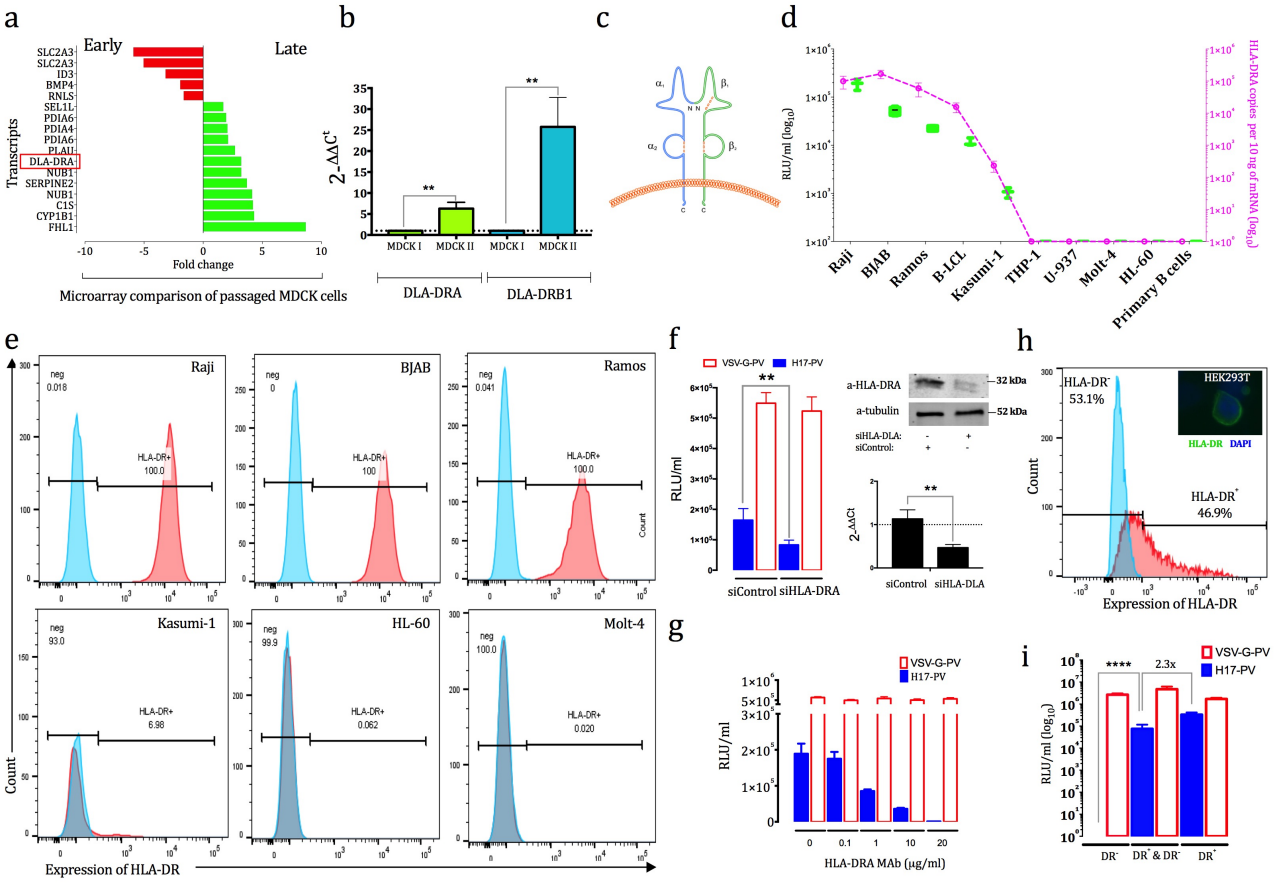

Supplementary material

Supplementary Material 1: List of cell lines included in the study.

Cell line	Type of cells	Species	Origin
Raji	Burkitt's lymphoma mature B-cells	Human	ATCC CCL-86
Ramos	Burkitt's lymphoma mature B-cells	Human	ATCC CRL-1596
BJAB	Burkitt's lymphoma mature B-cells	Human	CVCL_5711
HL-60	Promyeloblasts	Human	ATCC CCL-240
Molt-4	T lymphoblasts	Human	ATCC CRL-1582
Jurkat	T lymphocytes	Human	ATCC TIB-152
U-937	Monocytic leukemia	Human	ATCC CRL-1593.2
THP-1	Monocytic lymphoma	Human	ATCC TIB-202
B-LCLs	B-lymphoblastoid	Human	DOI: 10.1093/nar/gkw1167
Kasumi-1	Myeloblasts	Human	ATCC CRL-2724
Tb1 Lu	Epithelial lung	*Tadarida brasiliensis*	ATCC CCL-88
S. lilium lung	Lung	*Sturnira lilium*	Adolfo-Garcia Sastres & Martinez (The Icahn School of Medicine at Mount Sinai,NY, USA)/Aguilera's labs (Univ. of Costa Rica)
S. lilium kidney	Kidney	*Sturnira lilium*	
Ar. literatus lung	Lung	*Artibeus literatus*	
C. perspic kidney	Kidney	*Carollia perspicillata*	
C. perspic lung	Lung	*Carollia perspicillata*	
C. perspic liver	Liver	*Carollia perspicillata*	
PakiT03 cells	Epithelial kidney	*Pteropus Alecto*	Linfa Wang lab, NUS DOI: 10.1371/journal.pone.000826
PaBr cells	Brain	*Pteropus Alecto*	
A549 cells	Epithelial lung	Human	ATCC CRM-CCL-185
BEAS-2B	Epithelial lung/bronchus	Human	ATCC CRL-9609
HFF-1	Skin fibroblasts	Human	ATCC SCRC-1041
HeLa	Epithelial cervix	Human	ATCC CCL-2
HeLa S3	Epithelial cervix	Human	ATCC CCL-2.2
Caco-2	Epithelial colon	Human	ATCC HTB-37
HEK293T17	Kidney	Human	ATCC CRL-11268
DF-1	Embryo fibroblast	Chicken	ATCC CRL-12203
HD11	Macrophages	Chicken	CVCL_4685
CEF	Embryo fibroblasts	Chicken	The Pirbright Institute, UK
CER	Embryo-related	Chicken	DOI: 10.1016/j.biologicals.2005.08.001
Ou2	Fibroblasts	Chicken	CVCL_Y589
HD6	Erythroblasts	Chicken	PMCID: PMC230774

HP46	ALV-carcinoma	Chicken	PMCID: PMC361083
Cu447	Tumor cell line	Quail	DOI:10.1637/7182-032604R
Cu453	Tumor cell line	Quail	DOI:10.1637/7182-032604R
QT35	Muscle fibroblasts	Quail	ECACC:93120832
NMuMG	Mammary gland	Mouse	ATCC CRL-1636
LTK-11	Fibroblasts	Mouse	ATCC CRL-10422
BS-C-1	Kidney epithelial	Monkey	ATCC CCL 26
PK-15	Kidney epithelial	Pig	ATCC CCL-33
Wg3HCL2	HGPRT-Chinese hamster fibroblasts	Hamster	DOI: 10.1186/1297-9686-34-4-521
BHK-21	Kidney fibroblass	Hamster	ATCC CCL-10
CHO 1-15	Ovary epithelial	Hamster	ATCC CRL-9606
NBL-2	Epithelial kidney	Canine	ATCC CCL-34
MDCK I	Epithelial kidney	Canine	EEACC 00062106
MDCK II	Epithelial kidney	Canine	EEACC 00062107

Supplementary Material 2: List of the differentially regulated genes determined by microarray comparison between early and late passaged MDCK cells, as summarised in Fig. 2a. The encoded proteins of the differentially regulated transcripts were surveyed for their subcellular localisation (with the DeepLoc server) and presence of transmembrane domains (using the PHOBIUS and TMHMM algorithms).

Affymetrix ID	Refseq ID	Gene symbol	Gene name	Subcellular localisation (DeepLoc server)	Predicted transmembrane domains		FDR	Fold change
					TMHMM server	Phobius server		
Cfa.12195.3.S1_at	XM_003435535 XM_005641862 XM_014111636 XM_861215	FHL1	Four and a half LIM domains 1	Nucleus, Soluble	0		2.63E-05	8.68212
CfaAffx.10229.1.S1_at	NM_001159684	CYP1B1	Cytochrome P450, family 1, subfamily B, polypeptide 1	Endoplasmic reticulum, Membrane	0		1.28E-05	4.30944
Cfa.10821.1.A1_s_at	XM_005637210 XM_848227	C1S	Complement component 1, s subcomponent	Extracellular, Soluble	0		4.36E-06	4.21145

Cfa.12556.1.A1_at	XM_014119919	NUB1	Negative regulator of ubiquitin-like proteins 1	Cytoplasm, Soluble	0		2.01E-05	4.14298
Cfa.4394.1.S1_at	XM_014111110	SERPINE2	Serpin peptidase inhibitor, clade E (nexin, plasminogen activator inhibitor type 1)	Extracellular, Soluble	0		2.01E-05	3.70338
Cfa.7284.1.A1_s_at	XM_014119919	NUB1	Negative regulator of ubiquitin-like proteins 1	Cytoplasm, Soluble	0		2.21E-05	3.22491
Cfa.6456.1.S1_at	NM_001011723 XM_005627066 XM_005627067	DLA-DRA	MHC class II DR alpha chain	Cell membrane, Membrane	1	221-241	2.77E-05	3.21344
Cfa.127.1.S1_s_at	NM_001194952	PLAU	Plasminogen activator, urokinase	Extracellular, Soluble	0	20-40	2.14E-05	2.69368
CfaAffx.6163.1.S1_at	XM_532876	PDIA6	Protein disulfide isomerase family A, member 6	Endoplasmic reticulum, Soluble	0		1.83E-05	2.10444
Cfa.4275.2.S1_at	XM_843145	PDIA4	Protein disulfide isomerase family A, member 4	Endoplasmic reticulum, Soluble	1		8.19E-06	2.05558

CfaAffx.6163.1.S1_s_at	XM_532876	PDIA6	Protein disulfide isomerase family A, member 6	Endoplasmic reticulum, Soluble	0		8.36E-06	1.9391
CfaAffx.26500.1.S1_s_at	XM_014116111 XM_537530	SEL1L	Sel-1 suppressor of lin-12-like (C. elegans)	Endoplasmic reticulum, Membrane	1	768-786	5.15E-06	1.69924
Cfa.12560.1.A1_at	XM_005636642 XM_014108134 XM_847958 XR_001314613 XR_001314614	RNLS	Renalase, FAD-dependent amine oxidase	Mitochondrion, Membrane	0		3.65E-07	-1.64221
CfaAffx.22914.1.S1_at	NM_001287170	BMP4	Bone morphogenetic protein 4	Nucleus, Soluble	0		2.56E-05	-1.93435
Cfa.64.1.S1_at	NM_001003025	ID3	Inhibitor of DNA binding 3, dominant negative helix-loop-helix protein	Nucleus, Soluble	0		3.38E-06	-3.17884
Cfa.825.1.S2_at	NM_001003308	SLC2A3	Solute carrier family 2 (facilitated glucose transporter), member 3	Cell membrane, Membrane	10	7-26, 62-85, 97-115, 121-142, 154-177, 183-205, 270-293, 305-326, 333-355, 361-379, 400-420, 426-448	6.71E-06	-5.03551

CfaAffx.21479.1.S1_at	NM_001003308	SLC2A3	Solute carrier family 2 (facilitated glucose transporter), member 3	Cell membrane, Membrane	10	7-26, 62-85, 97-115, 121-142, 154-177, 183-205, 270-293, 305-326, 333-355, 361-379, 400-420, 426-448	2.21E-05	-5.89883

Supplementary Material 3: The ectodomain of HLA-DRA is well conserved in bats, humans and canine.

Multiple amino acid sequence alignment of canine DLA-DRA (NP_001011723.1), human HLA-DRA (NP_061984.2), and their bat orthologues [(Yinpterochiroptera *Pteropus alecto* (XP_006907484.1) and Yangochiroptera *Desmodus rotundus* (XP_024413747.1)]. *Desmodus rotundus* (common vampire bat) was chosen as the closest species to *Sturnira lilium* with a decoded genome. The alignment was performed by importing the corresponding amino acid sequences into CLC Workbench (CLC Bio, Qiagen, Aarhus, Denmark). Orange arrows indicate the ectodomain of the protein. Matrix below shows overall, pairwise amino acid similarity of HLA-DRA between the four species. The percent amino acid similarity values were calculated with the CLC workbench program.

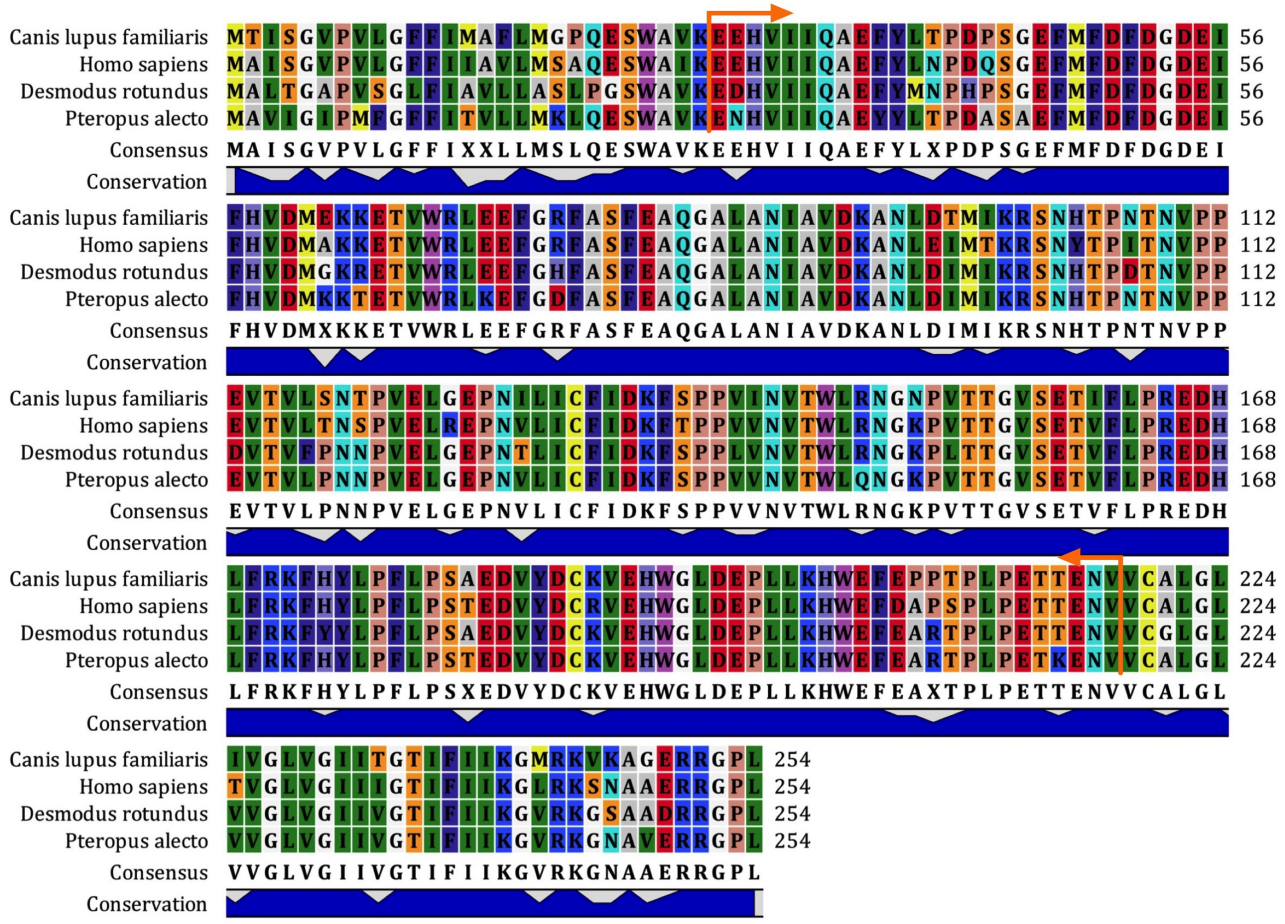

	1	2	3	4
Canis lupus familiaris				
1		89.01	88.48	89.53
Homo sapiens				
2	89.01		86.39	87.96
Desmodus rotundus				
3	88.48	86.39		89.01
Pteropus alecto				
4	89.53	87.96	89.01	

744

745 **Supplementary Material 4: Transfection of HEK293T/17 with HLA-DR α and β chains**
746 **results in surface expression of the heterodimer.**

747 HEK293T/17 cells were transfected with the empty vector or with HLA-DRA and DRB1
748 expression plasmids. The cells were fixed in paraformaldehyde and were permeabilised with
749 Triton X-100 to show intracellular distribution and immuno-stained with mAb HLA-DRA.
750 Nuclei were stained blue with DAPI stain (left panel), HLA-DR heterodimers were stained
751 green (middle panel), and the right panel shows a merged image. Fluorescent microscopy
752 analysis was performed with the EVOS FL fluorescent imaging system. Original magnification,
753 × 20.

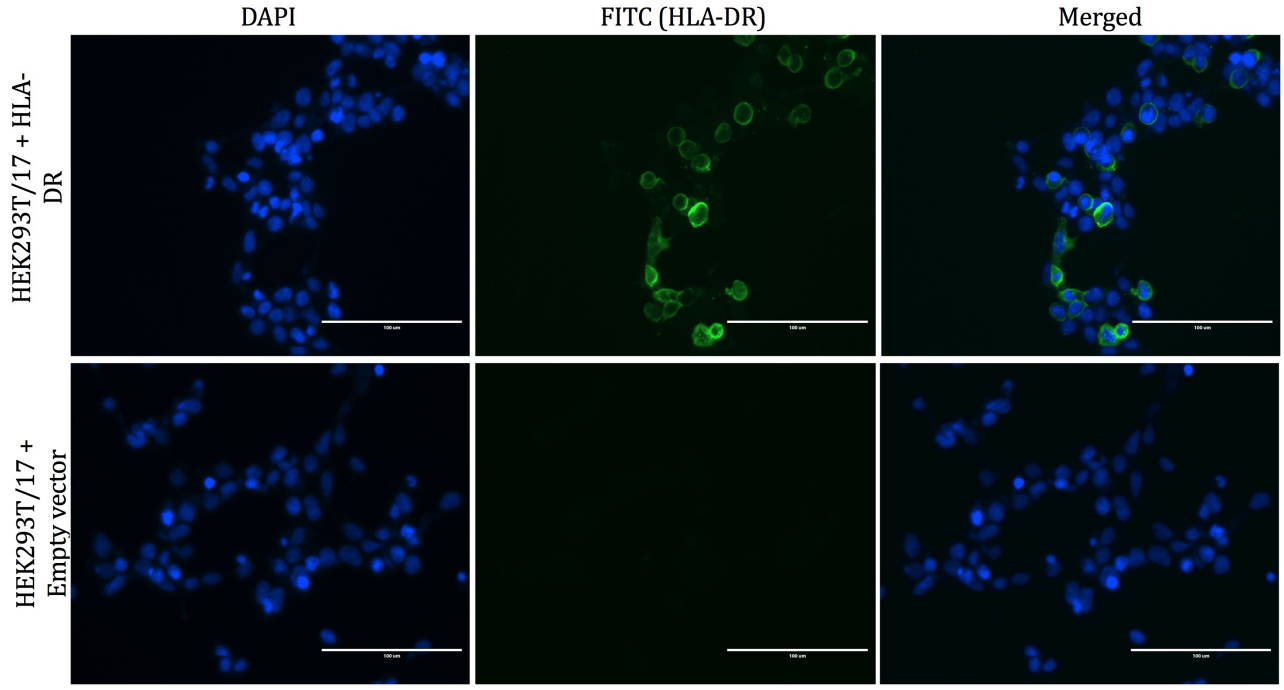

Supplementary Material 5: Transfection of bat PakiTO3 cells with HLA-DR α and β chains confers susceptibility to H17-PV.

Infectivity titers of H17-PV (RLU/ml) in PakiTO3 cells transfected for 48 h with equimolar amounts of either empty vector (pcDNA3.1) or the expression plasmid for HLA-DRA or the expression plasmids encoding both chains of HLA-DR. Cells were infected with PV for an extra 72 h in the presence of neomycin. Data represent mean values ± SEM of three independent experiments. One-way Anova with Dunnett *posthoc* test were used to analyse the data. ****$P<0.00005$ versus cells transfected with the empty vector.

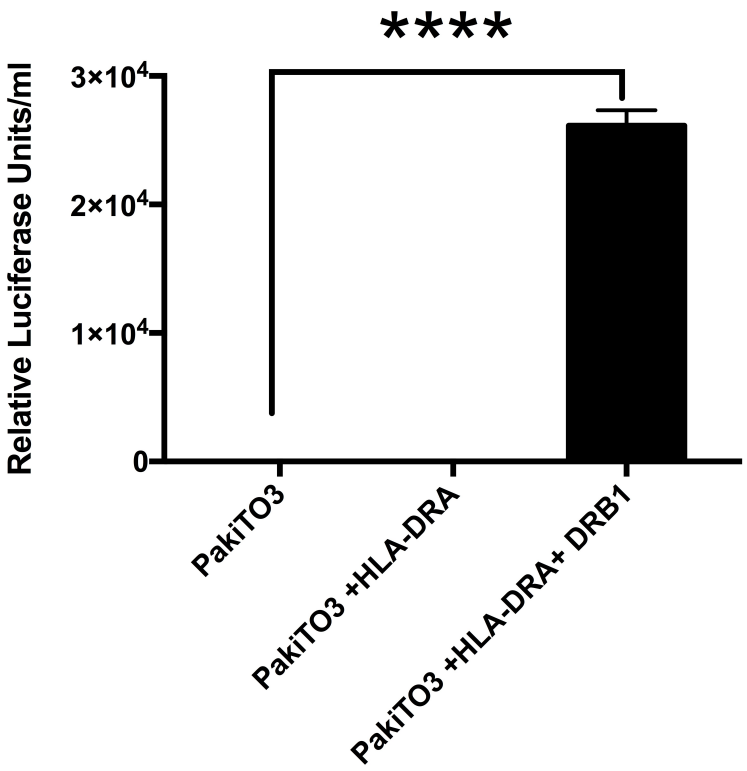

763